X International Conference on Computational Methods for Coupled Problems in Science and Engineering
COUPLED PROBLEMS 2023
M. Papadrakakis, B. Schrefler and E. Oñate (Eds)

IMPLICIT SCHUR COMPLEMENT ITERATIVE MODAL SOLVERS FOR MULTIPHYSICS MODEL ORDER REDUCTION

G. BURON[*,†], F. THOUVEREZ[*], L. JEZEQUEL[*], A. BELEY[†] AND F. THEVENON[†]

[*]Laboratoire de Tribologie et de Dynamique des Systèmes (LTDS)
Ecole Centrale de Lyon (ECL)
69134 Ecully, France
e-mail: guillaume.buron@ec-lyon.fr

[†]ANSYS France
69100 Villeurbanne, France

Key words: Schur complement, Multiphysics, Finite Element Method, Reduced Order Model, Eigensolvers, Piezoelectricity

Abstract. In this work, we propose iterative modal solvers to generate multiphysics finite element reduced order models. We consider the strongly coupled problems defined through differential-algebraic equations with sparse discrete operators. Piezoelectric models are common examples of such problems.

The approach we propose is based on the *Model Order Reduction (MOR) after Implicit Schur* method [1] which is used for the Krylov subspace reduction of piezoelectric devices. While their work uses the knowledge of the loading applied to the model to generate a Krylov subspace reduction basis, we propose to build a reduction basis with a priori unknown loading by modal synthesis. The basis is built from the eigenvectors of the problem after the static condensation by Schur complement of one of the physics. Typically, the Schur complement matrix is computed explicitly and it leads to dense operators [2] which limit the problem scales that can be studied due to large memory requirements and costly computations for the eigensolver used afterward.

For Krylov-based eigensolvers, the most computationally difficult step is to obtain a basis spanning the eigenspace of the problem on the considered eigenvalue range. By generalizing the *MOR after Implicit Schur* method, this basis can be constructed by an iterative procedure using the original sparse operators instead of the dense condensed operators. The original model may be significantly larger compared to the condensed model for typical cases. However, keeping the sparsity is a critical computational advantage for the considered problems. This method is minimally intrusive for the eigensolvers that only require the implementation of a matrix-vector product. Comparing this implicit Schur complement approach to the explicit Schur complement approach shows large computational cost reductions. It also underlines the problem scale limitations of the explicit approach even on high performance computing hardware.

1 INTRODUCTION

Industrial applications nowadays often involve the study of structural dynamics in a multiphysics environment. From microelectromechanical systems to large actuators, piezoelectricity is a typical example of such coupling. Piezoelectricity is commonly modeled in commercial software by strongly coupled finite element formulations, implemented in monolithic solvers. The use of finite element industrial models with millions of degrees of freedom is becoming more and more common. With the digital twin paradigm, the trend is toward increasingly larger problem sizes and more complex models. In this context, superelements are required not only to speed up computations, but also to enable a substructuring approach where complex models are partitioned into multiple components for design and efficiency reasons. It is common to simplify piezoelectric problems into structural-only problems using static condensation, thus we can apply structural superelement methods to piezoelectric models. As described by Jézéquel [3], there are numerous and varied substructuring methods. The typical structural superelements are listed in [4]. The Hurty/Craig-Bampton method [5, 4] is one method widely used in the industry. It uses modal synthesis to reduce most of the domain while keeping in physical space a smaller subdomain of master nodes. We can leverage its robustness and existing software implementations to reduce piezoelectric problems.

To achieve static condensation of the electric unknowns, we perform a Schur complement on the piezoelectric stiffness matrix. In the general case, the resulting Schur complement matrix is dense. Generating a Hurty/Craig-Bampton superelement after static condensation requires the computation of the first eigenvectors of a generalized eigenproblem involving the Schur complement matrix. The straightforward approach is to explicitly compute the Schur complement matrix and solve the dense eigenproblem. For the problem sizes that warrant Model Order Reduction (MOR), the computational cost and memory requirements of the reduction procedure are prohibitive. For large industrial models, this procedure is impossible with current High Performance Computing (HPC) hardware.

In the context of the Krylov subspace reduction of microelectromechanical devices, Hu et al. [1] proposed the *MOR after Implicit Schur* method to circumvent the increased computational cost of the reduction procedure after static condensation. They proved that the same Krylov subspace can be generated without the need to explicitely perform the Schur complement. This implicit Schur approach uses the sparse matrices of the original piezoelectric problem and implicitly condenses the electric unknowns. Contrary to Krylov subspace reduction, modal synthesis is not based on a known load-case. However, the required modes can be computed by iterative eigensolvers that use Krylov subspaces with procedures like the Arnoldi, Lanczos or Krylov-Schur algorithms. In this study, we adapt their implicit Schur approach to Krylov-based eigensolvers by modifying the iteration operator used in their procedures. This is non-intrusive for matrix-free solver implementations.

We propose a generalization of the *MOR after Implicit Schur* approach to Krylov eigensolvers. We implement the proposed method in an existing matrix-free Krylov-Schur eigensolver. We use this implicit Schur eigensolver to extract the first modes of a piezoelectric oscillator after static condensation and with boundary conditions representative of a Hurty/Craig-Bampton superelement generation procedure. Efficiency and accuracy of the implicit Schur eigensolver are compared to the explicit Schur approach using a dense eigensolver from the reference LAPACK linear algebra library [6].

NOTATIONS

In this study, we write the scalars x, vectors $\mathbf{x}$ and matrices $\mathbf{X}$ related to a physical problem with the indices $(\cdot)^{\beta}_{\alpha,(k)}$. α refers to a specific geometric domain. β refers to a specific physics. (k) refers to the index of an element in a sequence. When two indices are juxtaposed, it refers to the input and output of the transformation. For example, $\mathbf{A}^{12}$ is a transformation coupling the physics 1 and 2, while $\mathbf{A}_{12}$ couples the geometric domains 1 and 2. Usually, we do not write the zero vector $\mathbf{0}$ and zero matrix $\mathbf{O}$ in block vectors and matrices to avoid a cluttered notation. We call *modal space* a graded space $\mathcal{M}(S_\lambda) := \bigoplus_{\lambda \in S_\lambda} E_\lambda$ of the λ-eigenspaces E_λ of an operator over a subset S_λ of its eigenvalues.

2 PIEZOELECTRIC FULL ORDER MODEL

Several formulations of piezoelectricity are commonly used. In this study, we consider a displacement and voltage (u, v) two-field formulation. We are interested in the typical symmetric finite element formulation as implemented in the Ansys Mechanical APDL solver [7]. The problem is assumed to be conservative. The Full Order Model (FOM) is the discrete problem

$$\begin{bmatrix} \mathbf{M}^{\mathrm{uu}} & \\ & \mathbf{O} \end{bmatrix} \begin{Bmatrix} \ddot{\mathbf{u}} \\ \ddot{\mathbf{v}} \end{Bmatrix} + \begin{bmatrix} \mathbf{K}^{\mathrm{uu}} & \mathbf{K}^{\mathrm{uv}} \\ \mathbf{K}^{\mathrm{uv}\intercal} & \mathbf{K}^{\mathrm{vv}} \end{bmatrix} \begin{Bmatrix} \mathbf{u} \\ \mathbf{v} \end{Bmatrix} = \begin{Bmatrix} \mathbf{f}^{\mathrm{u}} \\ \mathbf{f}^{\mathrm{v}} \end{Bmatrix} \tag{1}$$

$$\Leftrightarrow \mathbf{M} \begin{Bmatrix} \ddot{\mathbf{u}} \\ \ddot{\mathbf{v}} \end{Bmatrix} + \mathbf{K} \begin{Bmatrix} \mathbf{u} \\ \mathbf{v} \end{Bmatrix} = \mathbf{f}, \tag{2}$$

of size $n := n^{\mathrm{u}} + n^{\mathrm{v}}$, with n^{u} displacement unknowns $\mathbf{u}$ and n^{v} voltage unknowns $\mathbf{v}$. The $\mathbf{K}$ and $\mathbf{M}$ matrices are sparse thanks to the finite element formulation. Note that the mass matrix $\mathbf{M}$ is indefinite, and the stiffness matrix $\mathbf{K}$ is singular without boundary condition on the voltage field.

The generalized eigenproblem $(\mathbf{K}, \mathbf{M})$ (3) defines the modes of the FOM (1), with $\mathbf{\Lambda}$ its real spectrum, and $\mathbf{\Phi}$ its real eigenvectors. From the sequence of increasingly larger eigenvalues, we define $\mathbf{\Lambda}$ as the spectral matrix $\mathrm{diag}(\lambda_{(1)}, ..., \lambda_{(n)})$. From the corresponding sequence of column eigenvectors, we define $\mathbf{\Phi}$ as the modal matrix $\begin{bmatrix} \boldsymbol{\varphi}_{(1)} & \cdots & \boldsymbol{\varphi}_{(n)} \end{bmatrix}$.

$$\begin{bmatrix} \mathbf{K}^{\mathrm{uu}} & \mathbf{K}^{\mathrm{uv}} \\ \mathbf{K}^{\mathrm{uv}\intercal} & \mathbf{K}^{\mathrm{vv}} \end{bmatrix} \begin{bmatrix} \mathbf{\Phi}^{\mathrm{u}} \\ \mathbf{\Phi}^{\mathrm{v}} \end{bmatrix} = \begin{bmatrix} \mathbf{M}^{\mathrm{uu}} & \\ & \mathbf{O} \end{bmatrix} \begin{bmatrix} \mathbf{\Phi}^{\mathrm{u}} \\ \mathbf{\Phi}^{\mathrm{v}} \end{bmatrix} \mathbf{\Lambda} \tag{3}$$

$$\Leftrightarrow \mathbf{K}\mathbf{\Phi} = \mathbf{M}\mathbf{\Phi}\mathbf{\Lambda}. \tag{4}$$

The eigenvectors may be normalized to enforce either orthonormalization $\mathbf{\Phi}^{\intercal}\mathbf{\Phi} = \mathbf{I}$ or $\mathbf{M}$-orthogonality $\mathbf{\Phi}^{\intercal}\mathbf{M}\mathbf{\Phi} = \mathbf{I}$.

3 REDUCE ORDER MODEL

3.1 Electric static condensation

Piezoelectric problems like (1) can be simplified into structural problems by static condensation of the electric unknowns $\mathbf{v}$. For a conservative problem, this is an exact reduction because the electric subproblem only introduces algebraic equations to the differential-algebraic system.

This static condensation can be equivalently applied to the FOM (1) by Galerkin projection using the reduction basis of constraint modes

$$\mathbf{T} := \begin{bmatrix} \mathbf{I} \\ -\mathbf{K}^{\mathrm{vv}-1}\mathbf{K}^{\mathrm{uv}\mathsf{T}} \end{bmatrix}, \tag{5}$$

similar to Guyan reduction [8] in structural dynamics, or by the Schur complement

$$\mathbf{S}^{\mathrm{uu}} = \mathbf{K}^{\mathrm{uu}} - \mathbf{K}^{\mathrm{uv}}\mathbf{K}^{\mathrm{vv}-1}\mathbf{K}^{\mathrm{uv}\mathsf{T}} = \mathbf{T}^{\mathsf{T}}\mathbf{K}\mathbf{T}. \tag{6}$$

The structural condensed problem is then

$$\mathbf{T}^{\mathsf{T}}\mathbf{M}\mathbf{T}\ddot{\mathbf{u}} + \mathbf{T}^{\mathsf{T}}\mathbf{K}\mathbf{T}\mathbf{u} = \mathbf{T}^{\mathsf{T}}\mathbf{f} \tag{7}$$

$$\Leftrightarrow \mathbf{M}^{\mathrm{uu}}\ddot{\mathbf{u}} + \mathbf{S}^{\mathrm{uu}}\mathbf{u} = \mathbf{f}^{\mathrm{u}} - \mathbf{K}^{\mathrm{uv}}\mathbf{K}^{\mathrm{vv}-\mathsf{T}}\mathbf{f}^{\mathrm{v}} =: \underline{\mathbf{f}}^{\mathrm{u}}. \tag{8}$$

3.2 Superelement overview

The Hurty/Craig-Bampton superelement [5] is a widespread and well-understood superelement method in structural dynamics. Following this method after electric static condensation, the problem (8) can be partitioned into condensed unknowns $\mathbf{u}_c$ and interface master unknowns $\mathbf{u}_m$. This leads to the equivalent problem

$$\begin{bmatrix} \mathbf{M}^{\mathrm{uu}}_{cc} & \mathbf{M}^{\mathrm{uu}}_{cm} \\ \mathbf{M}^{\mathrm{uu}\mathsf{T}}_{cm} & \mathbf{M}^{\mathrm{uu}}_{mm} \end{bmatrix} \begin{Bmatrix} \ddot{\mathbf{u}}_c \\ \ddot{\mathbf{u}}_m \end{Bmatrix} + \begin{bmatrix} \mathbf{S}^{\mathrm{uu}}_{cc} & \mathbf{S}^{\mathrm{uu}}_{cm} \\ \mathbf{S}^{\mathrm{uu}\mathsf{T}}_{cm} & \mathbf{S}^{\mathrm{uu}}_{mm} \end{bmatrix} \begin{Bmatrix} \mathbf{u}_c \\ \mathbf{u}_m \end{Bmatrix} = \begin{Bmatrix} \underline{\mathbf{f}}^{\mathrm{u}}_c \\ \underline{\mathbf{f}}^{\mathrm{u}}_m \end{Bmatrix}. \tag{9}$$

In the Hurty/Craig-Bampton method, the condensed unknowns $\mathbf{u}_c$ are reduced by modal synthesis with the fixed-interface boundary condition $\mathbf{u}_m := \mathbf{0}$. This requires the computation of the first normal modes $(\mathbf{\Lambda}^{\mathrm{u}}_c, \mathbf{\Phi}^{\mathrm{u}}_c)$ which are solutions to the generalized eigenproblem

$$\mathbf{S}^{\mathrm{uu}}_{cc}\mathbf{\Phi}^{\mathrm{u}}_c = \mathbf{M}^{\mathrm{uu}}_{cc}\mathbf{\Phi}^{\mathrm{u}}_c\mathbf{\Lambda}^{\mathrm{u}}_c. \tag{10}$$

4 SCHUR COMPLEMENT

4.1 Explicit Schur complement

The mass matrix $\mathbf{M}^{\mathrm{uu}}$ of the condensed problem (8) is sparse. However, its loaded stiffness matrix is the Schur complement matrix $\mathbf{S}^{\mathrm{uu}}$ and is shown by Kudryavtsev et al. [2] to be a dense matrix for piezoelectric models. Thus, the subproblem (10) to solve is also dense.

Because we need the first modes of (10) and not its dominant modes, the iterative eigensolvers based on the power iteration or subspace iteration methods cannot be used. The typical eigensolvers that can be used to extract the first modes of (10) will require at least a costly dense matrix factorization and dense linear solves involving the Schur complement matrix $\mathbf{S}^{\mathrm{uu}}_{cc}$.

Notable exceptions are LOBPCG-based eigensolvers [9, 10]. They do not require the matrix factorization of $\mathbf{S}^{\mathrm{uu}}_{cc}$. A matrix-free reprensation of $\mathbf{S}^{\mathrm{uu}}_{cc}$ could even be derived from (6), thus avoiding the explicit computation of the matrix and leveraging the sparsity of its constituents. However, the LOBPCG method is only efficient for the computation of very few modes. Generating a superelement generally requires the computation of too many modes for LOBPCG-based eigensolvers to be competitive. Moreover, the performance of LOBPCG-based eigensolvers is highly dependent on the preconditioner used and it is not trivial to find a good preconditioner that does not depend explicitly on the dense Schur complement matrix $\mathbf{S}^{\mathrm{uu}}_{cc}$.

4.2 Implicit Schur complement

Hu et al. [1] proved that the same Krylov subspace can be computed using the operators before (1) and after the static condensation (8). They used this property to propose the *MOR after Implicit Schur* method that performs efficiently the Krylov subspace reduction of their piezoelectric model. Although they are larger, using the original sparse matrices from (1) enables far better scalability compared to using the dense matrices from (8). This is significant because MOR is expected to be applied to very large models.

Because we are interested in component mode synthesis, we cannot apply the *MOR after Implicit Schur* method that requires a known external loading. Instead, we need the first modes of the eigenproblem (10). However, we note that eigenproblems of large sparse matrices are commonly solved by Krylov-based eigensolvers. Algorithm 1 is an overview of a Krylov-based eigensolver using the Arnoldi procedure [11].

Algorithm 1: Basic Arnoldi eigensolver.

input : operator $\mathfrak{O}$, starting vector $\mathbf{x}_{(0)}$ and direct eigensolver eig.
output: approximate modes $(\tilde{\mathbf{\Lambda}}, \mathbf{Q}\tilde{\mathbf{\Phi}})$ of operator $\mathfrak{O}$.

1 $\mathbf{q}_{(1)} \leftarrow \mathbf{x}_{(0)} / \left\|\mathbf{x}_{(0)}\right\|_2$
2 $\mathbf{Q} \leftarrow \left[\mathbf{q}_{(1)}\right]$ `// initialized Krylov subspace basis`
3 **for** $j \leftarrow 1$ **to** k **do**
4 $\quad \mathbf{x} \leftarrow \mathfrak{O}\,\mathbf{q}_{(j)}$ `// operator iteration`
5 $\quad$ **for** $i \leftarrow 1$ **to** j **do**
6 $\quad\quad h_{(ij)} \leftarrow \mathbf{x}^* \mathbf{q}_{(i)}$ `// Hessenberg coefficient`
7 $\quad\quad \mathbf{x} \leftarrow \mathbf{x} - h_{(ij)} \mathbf{q}_{(i)}$ `// orthogonalization`
8 $\quad h_{(j+1,j)} \leftarrow \|\mathbf{x}\|_2$ `// Hessenberg coefficient`
9 $\quad$ **if** $\|\mathbf{x}\|_2 = 0$ **then** `// breakdown check`
10 $\quad\quad$ break
11 $\quad$ **else**
12 $\quad\quad \mathbf{q}_{(j+1)} \leftarrow \mathbf{x} / \|\mathbf{x}\|_2$
13 $\quad\quad \mathbf{Q} \leftarrow \begin{bmatrix}\mathbf{Q} & \mathbf{q}_{(j+1)}\end{bmatrix}$ `// enriched Krylov subspace basis`
14 $\mathbf{H} \leftarrow \left[h_{(ij)}\right]$ `// Hessenberg matrix`
15 $(\tilde{\mathbf{\Lambda}}, \tilde{\mathbf{\Phi}}) \leftarrow \mathrm{eig}(\mathbf{H})$ `// small-scale direct eigensolve`
16 **return** $(\tilde{\mathbf{\Lambda}}, \mathbf{Q}\tilde{\mathbf{\Phi}})$

If we use the algorithm 1 to solve the eigenproblem (10) with the typical explicit Schur approach, the operator $\mathfrak{O}$ used in line 4 would be

$$\mathfrak{O} := -\mathbf{S}_{cc}^{\mathrm{uu}\,-1} \mathbf{M}_{cc}^{\mathrm{uu}}, \tag{11}$$

of size n^{u}. The algorithm would require an expensive matrix factorization of the dense Schur matrix $\mathbf{S}^{\mathrm{uu}}$ as well as k dense linear solves. In fact, this solver should not be used here.

Instead, we propose the implicit Schur approach with the modified operator

$$\mathfrak{O} := -\begin{bmatrix}\mathbf{I} & \mathbf{O}\end{bmatrix}\begin{bmatrix}\mathbf{K}_{cc}^{\mathrm{uu}} & \mathbf{K}_{cc}^{\mathrm{uv}} \\ \mathbf{K}_{cc}^{\mathrm{uv}\mathsf{T}} & \mathbf{K}_{cc}^{\mathrm{vv}}\end{bmatrix}^{-1}\begin{bmatrix}\mathbf{M}_{cc}^{\mathrm{uu}} & \\ & \mathbf{O}\end{bmatrix}\begin{bmatrix}\mathbf{I} \\ -\mathbf{K}_{cc}^{\mathrm{vv}-1}\mathbf{K}_{cc}^{\mathrm{uv}\mathsf{T}}\end{bmatrix}, \tag{12}$$

of size $n > n^{\mathrm{u}}$. While the rest of the eigensolver works in the structural subspace of $\mathbf{u}_c$ from the subproblem (10) to solve, we expand in line 4 to the multiphysics space of $\langle \mathbf{u}_c \quad \mathbf{v}_c \rangle^{\mathsf{T}}$ using constraint modes similar to those (5) of the global electric static condensation. This enables the use of sparse blocks from the matrices $\mathbf{K}$ and $\mathbf{M}$ of the original problem (1). While this space is larger, the sparsity should provide far better scalability. To restrict back to the subspace of the eigensolver, we just truncate the resulting vector to its structural part and discard its temporary constrained voltages. With this implicit Schur operator (12), the algorithm only requires the matrix factorization of the $\mathbf{K}_{cc}$ sparse block but also one more linear solve, although sparse, due to the constraint modes. However, because $\mathbf{M}_{cc}^{\mathrm{vv}} = \mathbf{O}$ for this piezoelectric problem, the operator could be further optimized by removing the constraint modes and only padding with zero voltages to expand the input space. While the explicit (11) and implicit (12) Schur operators are analytically equivalent, we expect some deviations in the modal results because the numerical operations are different.

Because the operator $\mathfrak{O}$ is only required at the line 4 of the algorithm 1 to evaluate the operator-vector product, it is possible to implement matrix-free eigensolvers for which the operator is defined outside of the solver. For such eigensolvers, implementing the implicit Schur approach is not intrusive.

5 NUMERICAL TEST CASE

5.1 Piezoelectric oscillator

We apply our implicit Schur approach to a piezoelectric oscillator and compare it to the explicit Schur approach. The model considered is a quartz tuning fork based on an example from the Ansys Mechanical APDL documentation [12]. The geometry is meshed with quadratic hexaedral piezoelectric elements from Mechanical APDL. The meshes considered are shown in figure 1. The problem sizes range from very small to quite large. To be consistent with the eigenproblem (10) of interest, we use the boundary conditions described by figure 2. The interface of master nodes is clamped $\mathbf{u}_m := \mathbf{0}$. A reference voltage $\mathbf{v}_0 := \mathbf{0}$ is applied as shown by the blue electrodes in figure 2. The rest of the unknowns are reduced. Among them, observation or control voltages $\mathbf{v}_e$, represented as the red electrodes in figure 2, could be kept in physical space but they are reduced to simplify the implementation of the methods. The condensed subdomain is then defined as

$$\left\langle \mathbf{u}_c \quad | \quad \mathbf{v}_c \right\rangle^{\mathsf{T}} := \left\langle \mathbf{u}_i \quad \mathbf{u}_0 \quad \mathbf{u}_e \quad | \quad \mathbf{v}_i \quad \mathbf{v}_e \quad \mathbf{v}_m \right\rangle^{\mathsf{T}}. \tag{13}$$

5.2 Computing setup

We use Ansys Mechanical APDL 2023R1 for modelling and meshing. We implement the explicit and implicit Schur approaches in Julia 1.8.5 [13] on a HPC server with 503 GB of RAM and two 20 cores/40 threads CPUs (Intel Xeon Gold 6138). All the BLAS/LAPACK linear algebra operations are performed using the widespread and optimized Intel Math Kernel Library

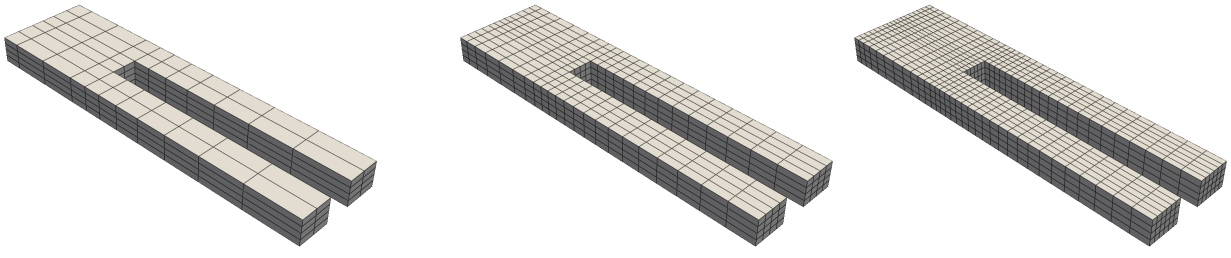

(a) $n = 4693$. (b) $n = 17\,041$. (c) $n = 37\,093$.

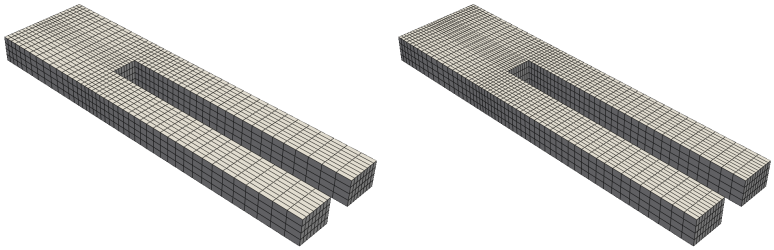

(d) $n = 64\,777$. (e) $n = 100\,237$.

Figure 1: Piezoelectric oscillator meshes of n degrees of freedom.

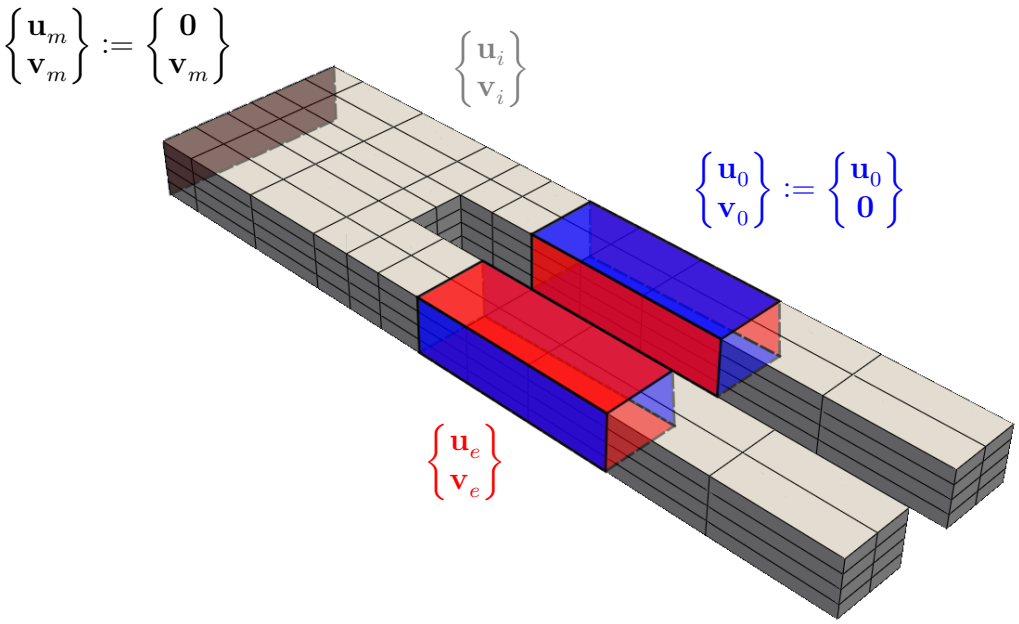

Figure 2: Piezoelectric oscillator partitioning and boundary conditions.

(MKL) 2022.2 wrapped in Julia. All the computations are performed in double precision with Shared Memory Parallelism on 24 threads (SMP24). We compute the first 48 modes of the eigenproblem (10).

To simplify the implementation of the explicit Schur approach, we compute the Schur complement matrix $\mathbf{S}_{cc}^{\mathrm{uu}}$ using the *simple* algorithm described in [14]. Because this is inefficient compared to optimized algorithms implemented in PARDISO [14] or MUMPS [15], the Schur complement cost is ignored to not skew the measured computational costs. However, this cost is significant for large problems even for optimized implementations. The dense eigenproblem (10) is solved using the reference linear algebra library LAPACK [6]. We use the LAPACK implementation from the MKL. We use the DSYGVX LAPACK eigensolver which is optimized for the computation of a small subset of modes of a symmetric generalized eigenproblem in double precision. We do not leverage the symmetry of the dense matrices to reduce their storage cost. However, this will not change the memory scalability of the approach and we observe that matrix storage only account for approximately 25% of the allocated memory for all the explicit Schur eigensolves performed in this study.

For the implicit Schur approach, we use the SuiteSparse library shipped with Julia 1.8.5 for all the sparse linear algebra operations. We use the matrix-free Krylov-Schur eigensolver from the ArnoldiMethod.jl 0.2.0 Julia package. The Krylov-Schur procedure [16] is a generalization of the Arnoldi procedure overviewed in algorithm 1.

5.3 Modal space similarity indicator

The common approach to quantify the similarity of two modal spaces is to compute the Modal Assurance Criterion (MAC) for each eigenvector pair of their eigenbases. However, we prefer to quantify directly the similarity between the two spaces instead of studying each vector of the bases. This is motivated by the fact that the same modal space can be spanned by different eigenbases if at least one eigenvalue is repeated. To achieve that, we use the space similarity indicator proposed by Campanile et al. [17]. For a reference orthogonal eigenbasis $\boldsymbol{\Psi}$ and an orthogonal eigenbasis $\boldsymbol{\Theta}$, the modal space similarity indicator ζ between the modal spaces $\mathrm{span}(\boldsymbol{\Psi})$ and $\mathrm{span}(\boldsymbol{\Theta})$ is

$$\zeta := |\cos\delta| = \min_{\mathbf{a}} \max_{\mathbf{b}} |(\boldsymbol{\Theta}\mathbf{b})^{\mathsf{T}}\boldsymbol{\Psi}\mathbf{a}| = |(\boldsymbol{\Theta}\mathbf{b}_\star)^{\mathsf{T}}\boldsymbol{\Psi}\mathbf{a}_\star|, \tag{14}$$

where $\boldsymbol{\Psi}\mathbf{a}_\star \in \mathrm{span}(\boldsymbol{\Psi})$ is the direction of the reference modal space which has the worst approximation $\boldsymbol{\Theta}\mathbf{b}_\star \in \mathrm{span}(\boldsymbol{\Theta})$ at the irreducible angle δ. Using the Lagrange multpliers method, the indicator is efficiently computed as

$$\begin{cases} \boldsymbol{\Psi}^{\mathsf{T}}\boldsymbol{\Theta}\boldsymbol{\Theta}^{\mathsf{T}}\boldsymbol{\Psi}\begin{bmatrix}\boldsymbol{\phi}_{(1)} & \cdots & \boldsymbol{\phi}_{(m)}\end{bmatrix} = \begin{bmatrix}\boldsymbol{\phi}_{(1)} & \cdots & \boldsymbol{\phi}_{(m)}\end{bmatrix}\mathrm{diag}(\lambda_{(1)},...,\lambda_{(m)}) \\ \zeta = \sqrt{\lambda_{(1)}}. \end{cases} \tag{15}$$

5.4 Results

The meshes from figures 1d and 1e are not studied with the explicit Schur approach due to unreasonable computational costs. Considering the explicit Schur results as reference, table 1 demonstrates that both the spectrums and modal spaces computed with the implicit Schur approach are accurate.

Table 1: Implicit/explicit Schur accuracy for 48 modes.

full problem size n	max eigenfrequency deviation (%)	modal space similarity ζ (%)
4693	0.310	99.996
17 041	0.286	99.998
37 093	0.270	99.998

Regarding scalability, the figure 3 shows far better scalability in execution time for the implicit Schur approach. Here, the explicit Schur appproach scales in $n^{2.9}$ while the implicit Schur scales in $n^{1.8}$. Despite not accounting for the Schur complement cost in the explicit Schur approach, the implicit Schur approach is faster at all problem sizes. As expected of a dense approach, the figure 4 shows poor scalability in memory usage for the explicit Schur approach. Here, the explicit Schur memory usage is quadratic while the implicit Schur is linear. Varying the number of threads leads to similar trends.

These results demonstrate that the explicit Schur approach is unsuitable for large models. The good scalability observed with the implicit Schur approach is promising and very large scale problems should be reachable with distributed memory parallelism which is often implemented for Krylov-based sparse eigensolvers.

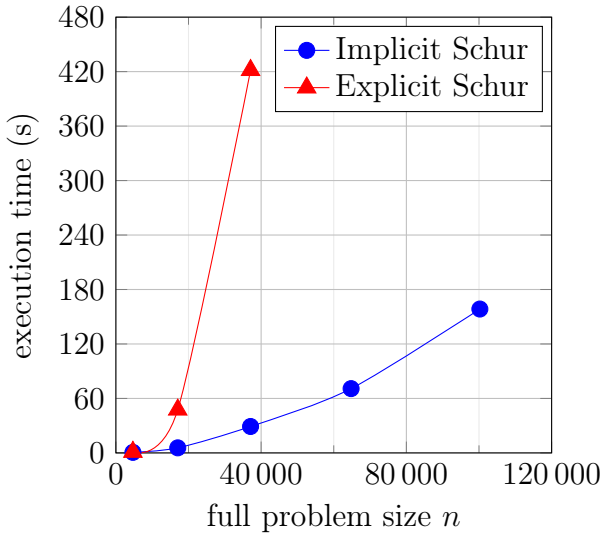

Figure 3: Time to extract 48 modes in SMP24.

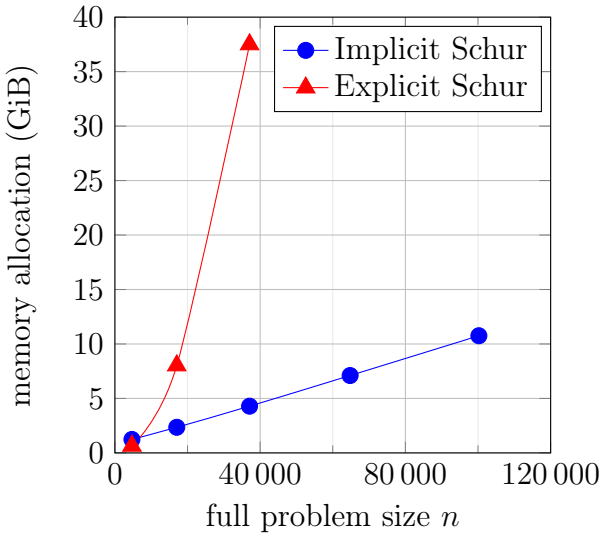

Figure 4: Memory usage to extract 48 modes in SMP24.

Using the MAC, we observe that all the explicit and implicit Schur eigenvectors are similar except for the modes 25, 26, 35 and 36 as described by table 2. Because the modal spaces are similar as shown in table 1, this should be caused by mode multiplicity and not by error on the modal results. The gaps between the eigenvalues of the pairs $(\lambda_{(25)}, \lambda_{(26)})$ and $(\lambda_{(35)}, \lambda_{(36)})$ are less than 1%, which is inconsistent with the modal density of the rest of the spectrum. This suggests that $\lambda_{(25)} = \lambda_{(26)}$ and $\lambda_{(35)} = \lambda_{(36)}$ are repeated eigenvalue pairs. However, comparing visually the eigenvector 35 figure 5a and eigenvector 36 figure 5b shows no obvious symmetry

typical of repeated modes.

$$\forall(\gamma,\mu)\in\mathbb{R}^2,\ \max_{(\alpha,\beta)\in\mathbb{R}^2}\mathrm{MAC}(\gamma\boldsymbol{\Psi}_{(\mathrm{I})}+\mu\boldsymbol{\Psi}_{(\mathrm{II})},\alpha\boldsymbol{\theta}_{(\mathrm{I})}+\beta\boldsymbol{\theta}_{(\mathrm{II})})>99.9\%. \tag{16}$$

By numerical validation of the relation (16) between the explicit Schur $(\boldsymbol{\Psi}_{(\mathrm{I})},\boldsymbol{\Psi}_{(\mathrm{II})})$ and implicit Schur $(\boldsymbol{\theta}_{(\mathrm{I})},\boldsymbol{\theta}_{(\mathrm{II})})$ eigenvector pairs, we observe that the modes (25, 26) and (35, 36) are in fact repeated modes. The eigenspaces $E_{\lambda_{(25)}=\lambda_{(26)}}$ and $E_{\lambda_{(35)}=\lambda_{(36)}}$ from the explicit and implicit Schur approaches are similar as predicted by the modal space indicator. This shows the advantage of the modal space indicator instead of relying directly on the MAC of the eigenvectors even when no trivial symmetry of the model is identified. The multiplicities observed are probably caused by symmetries in the underlying electric subproblem before static condensation.

Table 2: Low similarity of some eigenvectors for the mesh of figure 1c.

mode number	25	26	35	36
MAC (%)	99.626	99.569	98.573	98.088

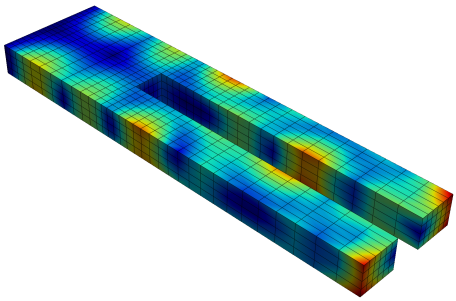

(a) Explicit Schur eigenvector 35.

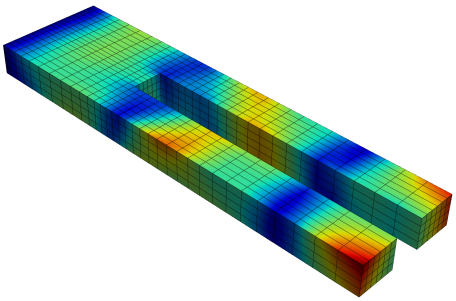

(b) Explicit Schur eigenvector 36.

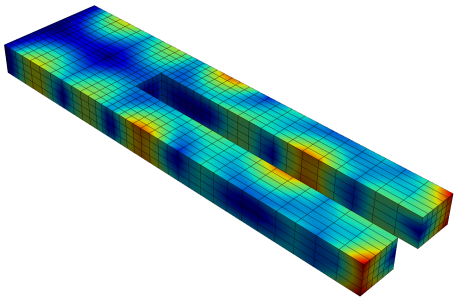

(c) Implicit Schur eigenvector 35.

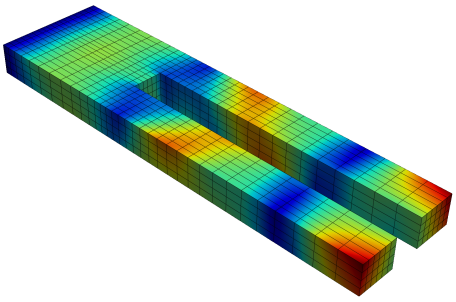

(d) Implicit Schur eigenvector 36.

Figure 5: Displacement magnitude of eigenvectors 35 and 36 from the implicit and explicit Schur approaches for the mesh of figure 1c.

6 CONCLUSIONS

This study shows that superelements of large piezoelectric models cannot be generated after electric static condensation using the straightforward explicit Schur complement. We generalized the work of Hu et al. [1] to propose an implicit Schur complement approach. For realistic numerical tests, the proposed implicit Schur approach demonstrates its accuracy as well as good scalability for the computation of normal modes. This enables superelement generation after electric static condensation for large conservative piezoelectric models using the well-understood substructuring methods. The implicit Schur approach uses existing Krylov-based eigensolvers and is minimally intrusive for matrix-free eigensolvers. To generate piezoelectric superelements of very large models, a distributed memory parallelism implementation of the implicit Schur approach is required. This implementation is possible because only common linear algebra operations are used.

Only conservative piezoelectricity is considered in this study, however the application of the implicit Schur approach to other multiphysics superelements is investigated. Moreover, differential-algebraic problems unrelated to multiphysics may benefit from the implicit Schur approach. To go further, a wide range of transformations instead of a simple static condensation can also be tested by capitalizing on the developed implicit strategy.

REFERENCES

[1] S. Hu, C. Yuan, A. Castagnotto, B. Lohmann, S. Bouhedma, D. Hohlfeld, and T. Bechtold. Stable reduced order modeling of piezoelectric energy harvesting modules using implicit Schur complement. *Microelectronics Reliability*, 85:148–155, June 2018.

[2] M. Kudryavtsev, E.B. Rudnyi, J.G. Korvink, D. Hohlfeld, and T. Bechtold. Computationally efficient and stable order reduction methods for a large-scale model of MEMS piezoelectric energy harvester. *Microelectronics Reliability*, 55(5):747–757, April 2015.

[3] L. Jézéquel. *Synthèse modale : théorie et extensions*. PhD thesis, Université Claude Bernard Lyon 1, 1985.

[4] Matthew S. Allen, Daniel Rixen, Maarten Van Der Seijs, Paolo Tiso, Thomas Abrahamsson, and Randall L. Mayes. *Substructuring in Engineering Dynamics: Emerging Numerical and Experimental Techniques*, volume 594 of *CISM International Centre for Mechanical Sciences*. Springer International Publishing, Cham, 2020.

[5] Roy R. Craig and Mervyn C. C. Bampton. Coupling of substructures for dynamic analyses. *AIAA Journal*, 6(7):1313–1319, July 1968.

[6] E. Anderson, Z. Bai, C. Bischof, S. Blackford, J. Demmel, J. Dongarra, J. Du Croz, A. Greenbaum, S. Hammarling, A. McKenney, and D. Sorensen. *LAPACK User's Guide Third Edition*. 1999.

[7] ANSYS Inc. *ANSYS 2023R1 Mechanical APDL Theory reference*. 2023.

[8] Robert J. Guyan. Reduction of stiffness and mass matrices. *AIAA Journal*, 3(2):380–380, February 1965.

[9] A. V. Knyazev. A Preconditioned Conjugate Gradient Method for Eigenvalue Problems and its Implementation in a Subspace. In K.-H. Hoffmann, H. D. Mittelmann, J. Todd, J. Albrecht, L. Collatz, P. Hagedorn, and W. Velte, editors, *Numerical Treatment of Eigenvalue Problems Vol. 5 / Numerische Behandlung von Eigenwertaufgaben Band 5*, volume 96, pages 143–154. Birkhäuser Basel, Basel, 1991. Series Title: International Series of Numerical Mathematics / Internationale Schriftenreihe zur Numerischen Mathematik / Série Internationale d'Analyse Numérique.

[10] Andrew V. Knyazev. Toward the Optimal Preconditioned Eigensolver: Locally Optimal Block Preconditioned Conjugate Gradient Method. *SIAM J. Sci. Comput.*, 23(2):517–541, January 2001.

[11] Z. Bai, J. Demmel, J. Dongarra, A. Ruhe, and H. van der Vorst. *Templates for the Solution of Algebraic Eigenvalue Problems: A Practical Guide*. SIAM, Philadelphia, 2000.

[12] ANSYS Inc. *ANSYS 2023R1 Mechanical APDL Coupled-Field Analysis Guide*. 2023.

[13] Jeff Bezanson, Alan Edelman, Stefan Karpinski, and Viral B. Shah. Julia: A Fresh Approach to Numerical Computing. *SIAM Rev.*, 59(1):65–98, January 2017.

[14] Alexander Kalinkin, Anton Anders, and Roman Anders. Schur Complement Computations in Intel Math Kernel Library PARDISO. *AM*, 06(02):304–311, 2015.

[15] Patrick Amestoy, I.S. Duff, Jean-Yves L'Excellent, and J. Koster. *MUltifrontal Massively Parallel Solver (MUMPS version 5.6.0) user's guide*. 2023.

[16] G. W. Stewart. A Krylov–Schur Algorithm for Large Eigenproblems. *SIAM J. Matrix Anal. & Appl.*, 23(3):601–614, January 2002.

[17] Lucio Flavio Campanile, S Kirmse, and Alexander Hasse. A measure for the similarity of vector spaces. Publisher: Unpublished, 2021.